Extending External Rays Throughout the Julia Sets of Rational Maps [*]

Figen Çilingir [†]
Robert L. Devaney
Elizabeth D. Russell

September 5, 2009

[*] 2000 MSC number: Primary 37F10; Secondary 37F45

[†] The first author would like to thank the Department of Mathematics at Boston University while this work was in progress. In addition, she would also like to thank TUBİTAK for their support while this research was in progress

External rays are an important tool in the study of the dynamics of complex polynomials of degree $n \geq 2$. For such maps, the point at ∞ is always a superattracting fixed point, and so we have an immediate basin of attraction of that fixed point. Near ∞, it is well known that the polynomial is conjugate to the simple map $z \mapsto z^n$. In the case where none of the finite critical points of the polynomial lie in this basin, then the conjugacy can be extended to the entire immediate basin of attraction. Then the image of the straight ray $t \mapsto te^{i\theta}, t > 1$, under this conjugacy is called the *external ray of angle* θ where θ is defined mod 1. It is known that many (though not necessarily all) of these external rays land on (i.e., have a unique limit point as $t \to 1$ at) a point in the boundary of the immediate basin which, in turn, is the Julia set of the polynomial. How these external rays land then provides a description of the topology of the Julia set of the polynomial.

In this paper we shall consider the analogous situation for the families of rational maps given by

$$F_\lambda(z) = z^n + \frac{\lambda}{z^n}.$$

These maps are special for several reasons. First, as in the case of complex polynomials, the point at ∞ is a superattracting fixed point, so we have an immediate basin of attraction. F_λ is again conjugate to $z \mapsto z^n$ near ∞, and, provided that none of the critical points lie in this basin, this conjugacy may be extended to the entire immediate basin of ∞. Thus we have the concept of external rays for these maps as well. For these maps, the origin is a pole, so we have a neighborhood of the origin that is mapped to the basin at ∞. If these two open sets are disjoint, then we may pull the external rays back to a neighborhood of the origin and then successively to the infinitely many other preimages of this set.

A second reason for the importance of these families is the fact that, as in the case of the well-studied quadratic family $z \mapsto z^2 + c$, there is only one free critical orbit (up to symmetry) for these maps. Moreover, these critical orbits may escape to ∞ under iteration of F_λ. Unlike the quadratic case, however, there are several different ways the critical orbits may escape. For example, if the critical orbits enter the immediate basin of ∞ at the second iteration, the Julia set is a Cantor set of concentric closed curves. If it takes more than two iterations for the critical orbits to escape, then the Julia set is a Sierpinski curve. See [4].

Our goal in this paper is to develop a method by which the external rays in the immediate basin of ∞ may be extended to the entire Julia set. In the case of polynomials, when the external rays can be extended to a Julia set that is connected, each extended ray always meets the Julia set in exactly one point, and several rays may sometimes land at the same point. How these rays land then provides an algorithm for descibing the dynamics on the Julia set via symbolic dynamics.

In our family of rational maps, the extended rays will be quite different — they will always meet the Julia set in a Cantor set of points and, in addition, they will pass through countably many different components of the Fatou set. These rays will each contain closed curves passing through the origin and ∞. The extended ray of angle θ will contain the external rays of angle θ and $\theta + 1/2$ and will be mapped two-to-one over the external ray of angle $n\theta$. Each extended ray will subdivide into a pair of dynamically distinct pieces. The first piece will lie in the Fatou set and will consist of a collection of arcs that lie in the immediate basin of ∞ and certain of its preimages. So all points on this portion of the extended ray have orbits that tend to ∞. The second portion is the complementary set which lies in the Julia set. This portion is always a Cantor set. This portion of the ray is then mapped onto the image Cantor set in a manner conjugate to the one-sided shift map on two symbols. Thus the extended rays allow us to decompose the dynamics of F_λ on the Julia set and the basin of ∞ into two "simpler" maps: the shift map of the Cantor set and the circle map $\theta \to n\theta$ on the complementary portion.

It turns out that the extended rays for the rational maps are quite different from those for polynomials in other ways as well. One difference is that each extended ray necessarily crosses infinitely many other extended rays. How and where these rays cross depend on the behavior of the critical orbits. Another difference is that these rays are not always simple curves; rather, again depending upon the behavior of the critical orbits, there may be rays that come with finitely or infinitely many different arcs attached.

As we shall show, the structure of the set of extended rays varies greatly depending on the topology of the Julia set. So our goal in this paper is to illustrate these differences by concentrating on three specific topological types of Julia sets. The first example is a map for which there is a component of the Fatou set that is disjoint from the full basin of ∞. In this case, the extended rays are all simple closed curves which cross at points that lie in both the Fatou and Julia sets. The second example is a map for which the Julia set is a Cantor set of simple closed curves. In this case, countably many of the extended rays have infinitely many smaller arcs attached, but these rays only meet at points in the Fatou set. The third example is a map for which the Julia set is a Sierpinski curve. In this case, infinitely many extended rays come with finitely many arcs attached, and the number of these attachments varies depending on the external angle of the ray.

As was shown in [5], there are infinitely many disjoint open sets of parameters in these families for which the Julia sets are Sierpinski curves but the dynamical behavior of maps drawn from different open sets is very different. In a subsequent paper, we plan to extend the construction of external rays to any Sierpinski curve Julia set to illustrate this different dynamical behavior.

Acknowledgement. This paper (as well as many of our previous papers) depends very heavily on ideas from both topology and nonlinear dynamical systems. Without the fundamental breakthroughs of Stephen Smale in these areas, this paper would not have been possible. We gratefully acknowledge his fundamental contributions in these areas.

1 Preliminaries

Let $F_\lambda(z) = z^n + \lambda/z^n$ where $\lambda \in \mathbb{C}$ is a parameter and $n \geq 2$. When $|z|$ is large, $F_\lambda(z) \approx z^n$, so F_λ has an immediate basin of attraction at ∞ that we denote by B_λ. As is well known [7], there is a Böttcher coordinate ϕ_λ that conjugates F_λ to $z \mapsto z^n$ in a neighborhood of ∞.

Each F_λ also has a pole of order n at the origin. Hence there is an open neighborhood of 0 that is mapped into B_λ. Now, either this neighborhood is disjoint from B_λ or else this neighborhood is contained in B_λ. In the former case, we denote the entire preimage of B_λ that contains the origin by T_λ. We call this region the *trap door* since any point $z \notin B_\lambda$ for which $F_\lambda^k(z)$ lies in B_λ for some $k > 0$ has the property that there is a unique point on the orbit of z that lies in T_λ.

Besides 0 and ∞, F_λ has $2n$ additional critical points given by $c_\lambda = \lambda^{1/2n}$. However, F_λ has only two critical values given by $v_\lambda = \pm 2\sqrt{\lambda}$. In fact, there is only one free critical orbit for F_λ up to symmetry. For, if n is even, we have $F_\lambda(2\sqrt{\lambda}) = F_\lambda(-2\sqrt{\lambda})$, so each of the critical orbits lands on the same point after two iterations. If n is odd, then we have $F_\lambda(-z) = -F_\lambda(z)$, so the orbits of $\pm 2\sqrt{\lambda}$ are symmetric under $z \mapsto -z$.

Recall that the *Julia set*, $J(F_\lambda)$, of the rational map F_λ has several equivalent characterizations. It is known that the Julia set is the closure of the set of repelling periodic points as well as the boundary of the set of points whose orbits tend to ∞ [7]. The complement of the Julia set is called the *Fatou set*.

There are several symmetries in the dynamical plane. First let $\nu = \exp(\pi i/n)$. Then we have $F_\lambda(\nu z) = -F_\lambda(z)$, so, as above, either the orbits of z and νz coincide after two iterations (when n is even), or else they behave symmetrically under $z \mapsto -z$ (when n is odd). In either event, the dynamical plane and the Julia set both possess $2n$-fold symmetry, as do B_λ and T_λ. Let $H_\lambda(z)$ be one of the n involutions given by $\lambda^{1/n}/z$. Then $F_\lambda(H_\lambda(z)) = F_\lambda(z)$, so the dynamical plane and Julia set are also symmetric under each H_λ. Note that $H_\lambda(B_\lambda) = T_\lambda$.

The following result is proved in [4].

Theorem *(The Escape Trichotomy). Let $F_\lambda(z) = z^n + \lambda/z^n$ with $n \geq 2$ and consider the orbit of v_λ.*

1. *If v_λ lies in B_λ, then $J(F_\lambda)$ is a Cantor set;*

2. *If v_λ lies in T_λ, then $J(F_\lambda)$ is a Cantor set of simple closed curves, each*

of which surrounds the origin;

3. *If $F_\lambda^k(v_\lambda)$ lies in T_λ with $k \geq 1$, then $J(F_\lambda)$ is a Sierpinski curve.*

In addition, if v_λ does not lie in either B_λ or T_λ, then $J(F_\lambda)$ is a connected set.

We remark that case 2 of the above result was proved by McMullen [6]. This part of the Theorem does not occur in the special case $n = 2$.

A *Sierpinski curve* is any planar set that is homeomorphic to the well-known fractal called the *Sierpinski carpet*. By a result of Whyburn [9], there is a topological characterization of such sets: any planar set that is compact, connected, locally connected, nowhere dense, and has the property that any pair of complementary domains are bounded by simple closed curves that are pairwise disjoint is known to be homeomorphic to the Sierpinski carpet. A Sierpinski curve also has the interesting property that it is a universal plane continuum in the sense that it contains a homeomorphic copy of any compact, connected, one-dimensional planar set.

We turn now to the parameter plane for these families, i.e., the λ-plane. Because of the Escape Trichotomy, the parameter plane divides into three distinct regions. Let $\mathcal{L}$ be the set of parameters for which $v_\lambda \in B_\lambda$ so $J(F_\lambda)$ is a Cantor set. We call $\mathcal{L}$ the *Cantor set locus*. Let $\mathcal{M}$ denote the set of parameters for which $v_\lambda \in T_\lambda$; $\mathcal{M}$ is called the *McMullen domain*. It is known that $\mathcal{M}$ is an open disk punctured at the origin and bounded by a simple closed curve [1]. Let $\mathcal{C}$ denote the complement of $\mathcal{L} \cup \mathcal{M}$. $\mathcal{C}$ is called the *connectedness locus* since $J(F_\lambda)$ is a connected set if $\lambda \in \mathcal{C}$. It is known that $\mathcal{C}$ contains precisely $(2n)^{k-3}(n-1)$ *Sierpinski holes* with escape time $k \geq 3$ (see [2], [8]). These are open disks in $\mathcal{C}$ in which each corresponding map has the property that the critical orbit lands in B_λ at iteration k or, equivalently, the critical orbit lands in T_λ at iteration $k-1$. See Figure 1.

In Figure 1, there are three clearly visible copies of the Mandelbrot set. Indeed, it is known that, for $n > 2$, there are $n-1$ copies of the Mandelbrot set that straddle the rays given by $\operatorname{Arg} \lambda = s\omega^k$ where $\omega^{n-1} = 1$ and $s > 0$ [3]. These sets are called the *principal Mandelbrot sets* in the parameter plane.

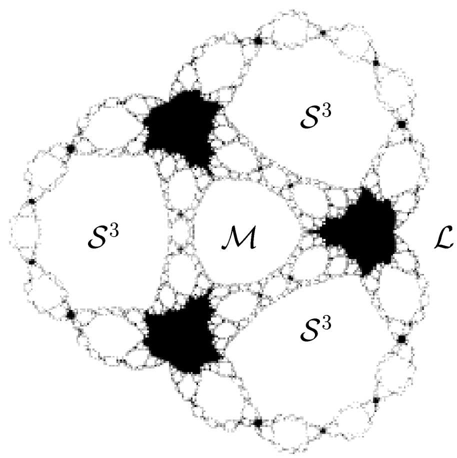

Figure 1: The parameter plane when $n = 4$. The open disks marked $\mathcal{S}^3$ are the Sierpinski holes with escape time 3.

The cusps of the main cardioids of these sets all lie on the boundary of $\mathcal{L}$ while the tips of the tails of these sets (i.e., the parameters corresponding to $c = -2$ in the usual Mandelbrot set for $z^2 + c$) all lie on the boundary of $\mathcal{M}$ (provided that $n > 2$). In addition, there are infinitely many other copies of the Mandelbrot set in $\mathcal{C}$ [2].

In our three examples of extending external rays, we shall choose one parameter from each of the McMullen domain, the principal Mandelbrot set, and a Sierpinski hole.

2 Parameters from the Principal Mandelbrot Sets

In this section we restrict attention to the family

$$F_\lambda(z) = z^2 + \frac{\lambda}{z^2},$$

though all of the results below go over in straightforward fashion to the more general families discussed above.

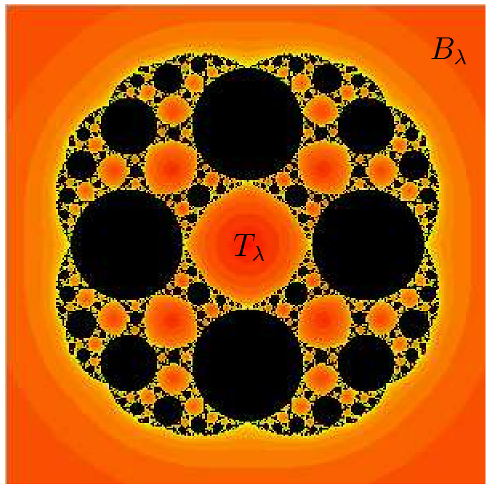

Figure 2: The Julia set for the map $z^2 + 1/16z^2$.

For simplicity, let $\lambda = 1/16$. This is the unique parameter for which the critical point $z_0 = 1/2$ is also a fixed point. The other three free critical points are given by $-1/2$ and $\pm i/2$; they all eventually map to z_0 and so are pre-fixed. We denote the immediate basin of attraction of z_0 by U_0. The Julia set for this map is depicted in Figure 2. The graph of $F_\lambda \,|\, \mathbb{R}$ shows that there is a second fixed point for F_λ on the positive real axis given by $p_\lambda \approx 0.9196$; this fixed point is repelling. We denote the preimage of this point on the positive real axis by u_λ. The graph of F_λ on $\mathbb{R}$ also shows that the entire open interval (u_λ, p_λ) lies in U_0. Similarly, $(p_\lambda, \infty]$ and $[\infty, -p_\lambda)$ lie in B_λ while $(-u_\lambda, u_\lambda)$ lies in T_λ.

One checks easily that the region $-U_0$ is mapped by F_λ two-to-one onto U_0 while the regions $\pm iU_0$ are mapped two-to-one onto $-U_0$ by F_λ and hence onto U_0 by F_λ^2. These are the four largest black disks in Figure 2. Since all of the free critical points map onto the fixed point z_0, it follows that F_λ is hyperbolic on its Julia set. We denote the boundaries of B_λ and T_λ by ∂B_λ and ∂T_λ. As shown in [4], ∂B_λ, ∂T_λ, and all of their preimages are simple closed curves. Similarly, the boundaries of U_0 and all of its preimages are simple closed curves. Note that no two of the preimages of the boundary of

B_λ ever touch. This follows since such an intersection point would necessarily be a critical point or one of its preimages, but we know that all of the free critical points eventually map into U_0, not ∂B_λ. In similar fashion, none of the preimages of the boundary of U_0 ever touch each other.

We now describe the structure of the Julia set of F_λ. We have two invariant simple closed curves in $J(F_\lambda)$, namely the boundaries of B_λ and U_0. F_λ is conjugate to $z \mapsto z^2$ on each of these simple closed curves, so repelling periodic points are dense in these two curves. However, there are no periodic points in any of the preimages of these two curves. Since repelling periodic points are well known to be dense in $J(F_\lambda)$, there must be (many) other points in $J(F_\lambda)$.

To describe the remainder of $J(F_\lambda)$, let A be the closed annulus separating B_λ and T_λ. Let Λ be the closed region given by A minus the union of $\pm U_0$ and $\pm iU_0$. Let I_0 be the closed subset of Λ contained in the quadrant $\text{Re}\, z \geq 0$ and $\text{Im}\, z \geq 0$. Let $I_1 = iI_0$, $I_2 = -I_0$, and $I_3 = -iI_0$. Note that I_0 meets I_3 in exactly two points, namely p_λ and u_λ. Similarly, $I_1 \cap I_2$ consists of the two preimages of p_λ lying in $\mathbb{R}^-$, and $I_0 \cap I_1$ and $I_2 \cap I_3$ also consist of a pair of points, each of which is mapped by F_λ onto $-p_\lambda$.

We have that $I_0 \cap \partial B_\lambda$ is mapped by F_λ onto the upper half of ∂B_λ, while $I_0 \cap \partial T_\lambda$ is mapped to the lower half of ∂B_λ. It follows that I_0 is mapped univalently over the entire region $\Lambda - (U_0 \cup -U_0)$ with the exception of the four "corner" points at which the map is two-to-one. The corner points p_λ and u_λ are both mapped to p_λ, while ip_λ and iu_λ are both mapped to $-p_\lambda$. The other I_j's are mapped in similar fashion over $A - (U_0 \cup -U_0)$ with a pair of corner points mapped to each of $\pm p_\lambda$

Let Σ_4 denote the space of one-sided sequences consisting of the four symbols $0, 1, 2,$ and 3. Given any point z in the Julia set of F_λ, we may associate an itinerary $S(z) \in \Sigma_4$ to z in the natural way: $S(z) = (s_0 s_1 s_2 \dots)$ where $s_j = k$ if $F_\lambda^j(z) \in I_k$. Note that there are some ambiguities in this definition of the itinerary since there are exactly eight points that lie in the intersection of two I_j's, namely $\pm p_\lambda, \pm ip_\lambda, \pm u_\lambda$, and $\pm iu_\lambda$. So each of these points has a pair of distinct itineraries associated to it. We therefore consider a modified sequence space Σ_4' in which certain itineraries are identified. We first make the identifications corresponding to the above eight points:

$$\begin{array}{ll} S(p_\lambda) = (\overline{0}) = (\overline{3}) & S(-p_\lambda) = (1\overline{3}) = (2\overline{0}) \\ S(u_\lambda) = (0\overline{3}) = (3\overline{0}) & S(-u_\lambda) = (1\overline{0}) = (2\overline{3}) \\ S(ip_\lambda) = (12\overline{0}) = (01\overline{3}) & S(-ip_\lambda) = (21\overline{3}) = (32\overline{0}) \\ S(iu_\lambda) = (11\overline{3}) = (02\overline{0}) & S(-iu_\lambda) = (22\overline{0}) = (31\overline{3}). \end{array}$$

See Figures 3 and 4 for the locations of the points with these itineraries. Then, if z is a point in the Julia set whose orbit eventually lands on one of these points, there are similarly two itineraries associated to this point, so we identify these two sequences as well.

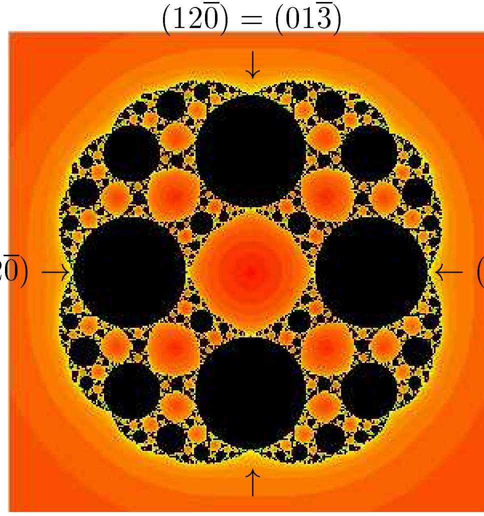

Figure 3: Points in ∂B_λ with identified itineraries.

After making these identifications, we endow Σ_4' with the usual topology. Then, using the fact that F_λ maps each I_j over all of the other I_k's, we have:

Proposition. *The map F_λ restricted to $J(F_\lambda)$ is topologically conjugate to the shift map on Σ_4'.*

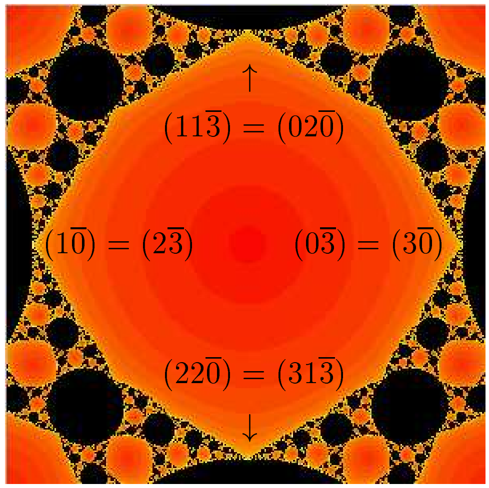

Figure 4: Points in ∂T_λ with identified itineraries.

In the sequel it will be important to understand the Σ_4'-itineraries of points that lie in the two invariant subsets of $J(F_\lambda)$ given by ∂U_0 and the boundary of ∂B_λ. Clearly, any point in ∂U_0 has itinerary that consists of only 0's and 3's. Conversely, since $F_\lambda \,|\, \partial U_0$ is conjugate to $z \mapsto z^2$, any such itinerary does correspond to a unique point in ∂U_0.

For points in ∂B_λ, the set of corresponding itineraries in Σ_4' is a little different from that corresponding to points in ∂U_0. If $z \in I_0 \cap \partial B_\lambda$, the first digit in the itinerary is 0, and the following digit in the itinerary of z must be either 0 or 1. Here we think of the points on the boundary of $I_0 \cap \partial B_\lambda$, namely p_λ and ip_λ, as having itineraries $(\overline{0})$ and $(01\overline{3})$ respectively, not $(\overline{3})$ or $(12\overline{0})$). That is, when we talk about an itinerary of a point in $I_0 \cap \partial B_\lambda$, such an itinerary will always begin with a 0. Similarly, itineraries of points in $I_2 \cap \partial B_\lambda$ begin with 2 and are followed by either 0 or 1. Points in $I_1 \cap \partial B_\lambda$ have itineraries that begin with 1 and are followed by either 2 or 3, while itineraries of points in $I_3 \cap \partial B_\lambda$ begin with 3 and are also followed by either 2 or 3. On the other hand, since $F_\lambda \,|\, \partial B_\lambda$ is conjugate to $z \mapsto z^2$, it follows that any itinerary that obeys these four rules corresponds to a point in ∂B_λ.

For later use, note that if $s = (s_0 s_1 s_2 \dots) \in \Sigma_4$ corresponds to a point in ∂B_λ, then, for each n, there is a unique odd and even integer that can follow each entry s_n. Now let $\Delta \subset \Sigma_4'$ be the sequence space corresponding to the subshift of finite type generated by the transition matrix

$$\begin{pmatrix} 1 & 1 & 0 & 0 \\ 0 & 0 & 1 & 1 \\ 1 & 1 & 0 & 0 \\ 0 & 0 & 1 & 1 \end{pmatrix}$$

modulo the identifications in Σ_4'. Then we have

Proposition. *The itinerary map $S : \partial B_\lambda \to \Delta$ is a homeomorphism that conjugates F_λ on ∂B_λ to the shift map on Δ.*

Consider now the set of one-sided sequences whose entries are just 0 and 1. Call this set Σ_2. We have a map $\pi : \Sigma_4 \to \Sigma_2$ given by $\pi(s_0 s_1 s_2 \dots) = (t_0 t_1 t_2 \dots)$ where $t_j = s_j \bmod 2$. So, for example, any sequence in Σ_4 which contains only 0's and 2's is mapped by π to the same sequence, namely $(\overline{0})$. Similarly any sequence in Σ_4 with only odd entries is mapped to $(\overline{1})$. We call a sequence in Σ_2 a *projected itinerary.* Note that certain points in $J(F_\lambda)$ may have several different projected itineraries. For example, the point p_λ has projected itinerary $(\overline{0})$ and $(\overline{1})$. Of importance later will be the set of points in $J(F_\lambda)$ that share the same projected itinerary.

Proposition. *Let $t \in \Sigma_2$. The set of points in $J(F_\lambda)$ whose projected itinerary is t is a Cantor set in $J(F_\lambda)$.*

Proof: Given the projected itinerary $t = (t_0 t_1 t_2 \dots)$, there are exactly two digits s_n that correspond to each digit t_n. So the set of sequences in Σ_4 that correspond to a given projected itinerary is homeomorphic to the sequence space on two symbols and hence to the Cantor set. No two points in this collection of points are identified since points that have two distinct itineraries in Σ_4 always have one itinerary that ends in all 0's and the other in all 3's (and so the projected itineraries of these sequences are different). Consequently, each of these sequences corresponds to a single point in $J(F_\lambda)$.

□

Proposition. *Let $t \in \Sigma_2$. Then there are exactly two sequences in Σ_4 that are mapped by π to t and for which the points in $J(F_\lambda)$ with the corresponding itineraries in Σ_4 lie in ∂B_λ. The corresponding points in ∂B_λ are negatives of one another and their itineraries in Σ_4 are of the form $(s_0 s_1 s_2 \dots)$ and $(\tilde{s}_0 s_1 s_2 \dots)$ where $\tilde{s}_0 \neq s_0$ but $\tilde{s}_0 = s_0 \bmod 2$.*

Proof: Let $z \in \partial B_\lambda$ and $S(z) = (s_0 s_1 s_2 \dots) \in \Sigma_4$. Suppose also that $t = (t_0 t_1 t_2 \dots) \in \Sigma_2$ satisfies $\pi(S(z)) = t$. If $t_0 = 0$, then we must have $s_0 = 0$ or $s_0 = 2$. We claim that the remainder of the sequence s is determined by this initial choice of s_0.

Suppose first that $s_0 = 0$. If $t_1 = 0$, then $s_1 = 0$ since the only even integer that may follow 0 in the sequence s is 0 since z lies in ∂B_λ, i.e., 2 cannot follow 0 for itineraries that correspond to points in ∂B_λ. If $t_1 = 1$, then we must have $s_1 = 1$ since, again, the only odd integer that may follow 0 is 1. Continuing in this fashion, we see that all subsequent entries of the sequence s are determined since there is a unique odd or even integer that follows any given s_n for points in ∂B_λ. Similar arguments hold when $s_0 = 2$ or $t_0 = 1$.

Now if $(s_0 s_1 s_2 \dots)$ is a sequence corresponding to a point $z \in \partial B_\lambda$, then the other such sequence must be $(\tilde{s}_0 s_1 s_2 \dots)$. This sequence then corresponds to $-z$ which, by symmetry, also lies in ∂B_λ.

□

We now proceed to define the extended rays for F_λ. Fix a projected itinerary $t \in \Sigma_2$. For each such t there will be a unique extended ray in $\overline{\mathbb{C}}$ denoted by ξ_t. Each extended ray will be a simple closed curve that passes through both the origin and ∞ in the Riemann sphere. F_λ will map each extended ray two-to-one onto the extended ray corresponding to the projected itinerary $\sigma(t)$ where $\sigma : \Sigma_2 \to \Sigma_2$ is the shift map,

To specify the points in ξ_t, we first expand the region in $\overline{\mathbb{C}}$ in which we define the itineraries of points. Let Q_0 denote the region in the Riemann sphere given by $\operatorname{Re} z \geq 0$ and $\operatorname{Im} z \geq 0$ minus the portions of the open sets

U_0 and iU_0 lying in this quadrant. We assume that both ∞ and the origin lie in Q_0. So Q_0 is a closed subset of $\overline{\mathbb{C}}$. Let $Q_1 = iQ_0$, $Q_2 = -Q_0$, and $Q_3 = -iQ_0$. With a slight abuse of terminology, we call each of these regions quadrants. So ∞ and 0 lie in all four of the quadrants. Note that F_λ maps each Q_j onto the entire Riemann sphere minus the two open disks $\pm U_0$. F_λ is univalent on the interior of each quadrant and takes the portions of Q_j on the real and imaginary axes two-to-one onto the portions of the real axis given by $[p_\lambda, \infty]$ and $[-\infty, -p_\lambda]$.

Recall that the involution $H_\lambda = \sqrt{\lambda}/z$ satisfies $F_\lambda(H_\lambda(z)) = F_\lambda(z)$. It follows that each H_λ maps Q_j with j odd to some Q_k with k even and vice versa.

We may now define exactly as before the itinerary $S(z) \in \Sigma_4$ as well as the projected itinerary $\pi(S(z)) \in \Sigma_2$ of any point z whose orbit remains for all iterations in the four quadrants Q_j, i.e., those points whose orbits never enter U_0. Again, as before, points may have a pair of associated itineraries. For example, any point in $\mathbb{R}^+$ that lies to the right of U_0 has itinerary either $(\overline{0})$ or $(\overline{3})$ while points that lie to the left of U_0 in $\mathbb{R}^+$ have itinerary either $(0\overline{3})$ or $(3\overline{0})$. We then define the *extended ray with itinerary* t to be the set of all points in $\overline{\mathbb{C}}$ whose projected itinerary is $t = (t_0 t_1 t_2 \ldots)$.

There are four types of points in each extended ray. First of all, 0 and ∞ belong to ξ_t for any sequence $t \in \Sigma_2$. Second, as shown above, given a projected itinerary t, there are a pair of points $\pm z_t$ in ∂B_λ that have this projected itinerary. Then, since the half-lines $(\pm p_\lambda, \infty]$ and $\pm i(p_\lambda, \infty]$ are external rays for F_λ landing at $\pm p_\lambda$ and $\pm i p_\lambda$, it follows that the external rays that land at the two points $\pm z_t$ also have projected itinerary t since these external rays cannot meet the four external rays above if $z_t \neq \pm p_\lambda, \pm i p_\lambda$. Note that the image of each of these two external rays is the external ray that lands at $F_\lambda(z_t)$. So there is a curve in T_λ that maps two-to-one onto the external ray that lands at $-F_\lambda(z_t)$. These curves are found by applying iH_λ to the two external rays landing at $\pm z_t$, and so points on this curve also have projected itinerary t. Third, there are points in the preimages of B_λ that remain in the $Q_j - B_\lambda$ for k iterations before landing in B_λ at the $(k+1)^{\text{st}}$

iteration. Points with this property move around the I_j's (and finally T_λ) with projected itinerary that begins $t_0 \dots t_k$. They then enter B_λ and land on the $(k+1)^{\text{st}}$ iterate of the external ray landing at $F_\lambda^{k+1}(\pm z_t)$. So these points also have projected itinerary t and thus lie in ξ_t. Finally, as also observed above, there is a Cantor set of points that lie in $J(F_\lambda)$ and in ξ_t.

Theorem. *The extended ray ξ_t is a simple closed curve in $\overline{\mathbb{C}}$ that passes through both* 0 *and* ∞ *and is mapped two-to-one onto the extended ray $\xi_{\sigma(t)}$.*

Proof: As mentioned above, the extended ray consists of points in a subset of the Julia set that is a Cantor set together with a pair of external rays and preimages of other external rays in B_λ. We claim that these subsets join up to form a simple closed curve passing through ∞ and 0. We first show that ξ_t is a connected set.

Let z_t be the landing point of one of the two external rays whose projected itinerary is t. Suppose that $S(z_t) = (s_0 s_1 s_2 \dots)$ where $\pi(S(z)) = t = (t_0 t_1 t_2 \dots)$. Let $V(s_j) = Q_{s_j} \cup Q_{\tilde{s}_j}$ where we recall that $\tilde{s}_j \neq s_j$ but $\tilde{s}_j = s_j \mod 2$. So the region $V(s_0)$ is a pair of closed "disks" that touch at exactly two points, 0 and ∞. Let $V(s_0 s_1) = V(s_0) \cap F_\lambda^{-1} V(s_1)$. Since F_λ is essentially univalent on each of the quadrants contained in $V(s_0)$, it follows that $F_\lambda^{-1} V(s_1) \cap Q_{s_0}$ is also a pair of disks that touch at the unique prepole in Q_{s_0} and also meet 0 and ∞. Therefore, $V(s_0 s_1)$ is a "string" of four "disks" connecting 0 to ∞. Each of these disks touches exactly two others and the intersection points are drawn from the set 0, ∞, and the two prepoles in $V(s_0)$. Continuing inductively, let $V(s_0 s_1 \dots s_n)$ denote the set $V(s_0) \cap F_\lambda^{-1}(V(s_1 \dots s_n))$. Then $V(s_0 \dots s_n)$ is a string of 2^n disks, each of which touches exactly two other disks at a unique point. This string of disks forms a "necklace" that passes through both 0 and ∞. We also have that the $V(s_0 \dots s_n)$ form a collection of nested, closed, and connected sets. Hence their intersection is a closed and connected set. But any point in this intersection must have projected itinerary given by $(t_0 t_1 t_2 \dots)$. Moreover, this set contains all points with this projected itinerary. Hence this intersection is ξ_t.

We next claim that this intersection is a simple closed curve. We know that there are two types of points in this intersection, the Cantor set of points in $J(F_\lambda)$ and the various preimages of external rays. Each of the preimages of external rays is a curve that meets exactly two points in the Cantor set portion of the set. We call these points "endpoints." So any particular curve accumulates on only two endpoints in $J(F_\lambda)$. Therefore the question is whether or not an infinite collection of such curves could limit on some point that is not in the Cantor set portion of ξ_t. But this cannot happen because the limiting point could not have orbit that escapes to ∞. Hence this orbit must be bounded. But the orbit of this point must then have projected itinerary t and so the point does indeed lie in the Cantor set portion of the set. Now this sequence cannot limit on more than one point in the Cantor set locus because the set of limit points of such a subsequence of curves would be a connected set. But the only connected components of a Cantor set are single points.

□

Note that all extended rays cross each other at 0 and at ∞. Let $\xi(t_0)$ be the set of all extended rays for which the first digit in the associated projected sequence is t_0. Then each of these rays cross at 0, ∞, and the two prepoles in the pair of quadrants associated with t_0, i.e., the first preimages of 0 in these quadrants. Now consider $\xi(t_0, t_1)$, the set of all extended rays for which the first two digits in the associated projected sequence are $t_0 t_1$. All of these rays cross at the previous four points together with four new points that are the second preimages of 0 that have the correct pair of digits in the first two places of their itinerary, i.e., their itineraries in Σ_4 begin with one of $(t_0 t_1)$, $(\tilde{t}_0, t_1)$, $(t_0, \tilde{t}_1)$, or $(\tilde{t}_0, \tilde{t}_1)$. Inductively, let $\xi(t_0, \ldots, t_k)$ be the set of extended rays for which the projected itinerary begins $t_0 t_1 \ldots t_n$. Then each ray in this set cross at a total of 2^{k+2} points, namely 0, ∞, and the appropriate preimages of 0.

Remarks:

1. Note that the external ray of angle 0 actually lies in two extended rays, namely ξ_t where $t = (\overline{0})$ and $t = (\overline{1})$. These two rays also meet along the

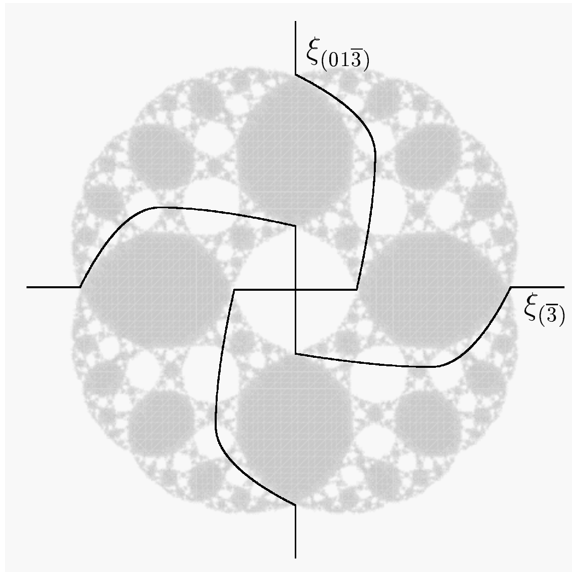

Figure 5: The extended rays ξ_t for $t = (\overline{3})$ and $(01\overline{3})$.

imaginary axis in T_λ, since these points are mapped to the negative real axis, i.e., the external ray of angle $1/2$.
2. Two extended rays also join up along any external ray of angle $k/2^n$. In this case, these rays also meet along arcs in T_λ as well as in the first $n-3$ preimages of T_λ that have the appropriate itineraries.
3. Each ξ_t also meets ∂U_0 in exactly one point, namely the point with itinerary $\hat{t} \in \Sigma_4'$, where $\hat{t}$ is the same as the projected itinerary t except all 1's are replaced by 3's. There is a similar single meeting point in the boundaries of each of $-U_0, iU_0$, and $-iU_0$.

As a consequence, the set of extended rays is quite intertwined as it makes its way from B_λ to T_λ. For a picture of some of the extended rays, see Figure 5.

3 A Parameter Drawn from the McMullen Domain

In this section, we restrict attention to the family

$$F_\lambda(z) = z^3 + \frac{\lambda}{z^3}.$$

(We choose $n = 3$ in this section since there is no McMullen domain when $n = 2$.) Again, for simplicity, we will study a specific example. In this case we choose $\lambda \in \mathbb{R}^+$. Results for any other λ value in the McMullen domain will be similar. The main difference here is that the critical points now lie in a preimage of the trap door and so the critical points will lie on certain extended rays. As a consequence, these special extended rays will no longer be simple closed curves but rather they will have certain branches attached.

For this map there are six critical points located at $\lambda^{1/6}$ and six prepoles (preimages of 0) at $(-\lambda)^{1/6}$. The prepoles and critical points all lie on the *critical circle* given by $|z| = |\lambda|^{1/6}$. The critical points map to the two critical values v_λ which are located at $\pm 2\sqrt{\lambda} \in \mathbb{R}$ and the critical circle is mapped six-to-one onto the line segment connecting the critical values. The straight line connecting 0 to ∞ and passing through a critical point is called a *critical ray.* The critical rays are each mapped two-to-one onto one of the straight lines $[\pm v_\lambda, \infty)$. These rays also divide the region between B_λ and T_λ into six subsets $I_0, \ldots, I_5$ which will play the same role as the I_j in the previous section. Also, the graph of F_λ on $\mathbb{R}$ shows that there are four real fixed points (see Figure 6 for the case $\lambda = .01$).

As described in the Escape Trichotomy, the Julia set of F_λ is a Cantor set of simple closed curves. As before, we have the immediate basin of ∞, B_λ. Since all of the critical orbits eventually end up in B_λ, the Julia set of F_λ is what remains after the immediate basin of ∞ and all its preimages have been removed. The first preimage is the trap door T_λ containing 0 and the two critical values. The preimage of the trap door is (via the Riemann-Hurwitz formula) an open annulus $\mathcal{A}$ that necessarily contains all of the critical points. Each subsequent preimage is then a pair of annuli that are both mapped as

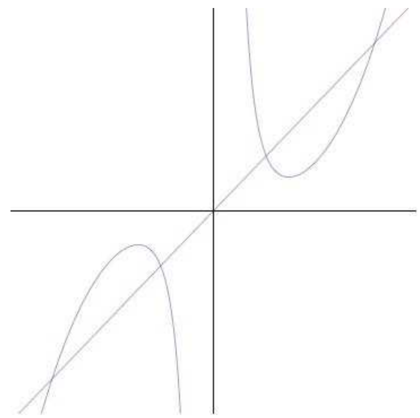

Figure 6: The graph of $F_{0.01}(x) = x^3 + 0.01/x^3$

three-to-one coverings onto their image annulus. The boundary curves of these annuli all surround 0.

We now define the extended ray of angle 0. Unlike the previous case, this ray will not be a simple closed curve passing through 0 and ∞. Rather, this ray will have infinitely many attachments. Since $\lambda \in \mathbb{R}^+$, the external ray of angle 0 lies in $\mathbb{R}^+$ and lands at the rightmost fixed point in $\mathbb{R}^+$. We may extend this ray to include the half line $[0, \infty]$. This line is then mapped two-to-one onto the line $[v_\lambda, \infty]$, so the original half line is not mapped onto itself. The segment of $\mathbb{R}^+$ that is not covered is the interval $[0, +v_\lambda)$. One checks easily that this entire interval lies in the trap door. There is then an arc α on the critical circle that connects the critical point on $\mathbb{R}^+$ to the prepoles in regions I_0 and I_5 and this arc is mapped two-to-one over the interval $[0, +v_\lambda)$. Then the set $\mathbb{R}^+ \cup \alpha$ is mapped in two-to-one fashion over itself except for the arc α. We may then adjoin two arcs, β_1 and β_2, lying in the two preimages of $\mathcal{A}$, and this will ensure that α is covered two-to-one. Continuing in this manner, we attach pairs of arcs that are mapped to the arcs added in the previous step of the construction. Thus, the extended 0 ray contains the positive real axis together with a countable set of arcs and

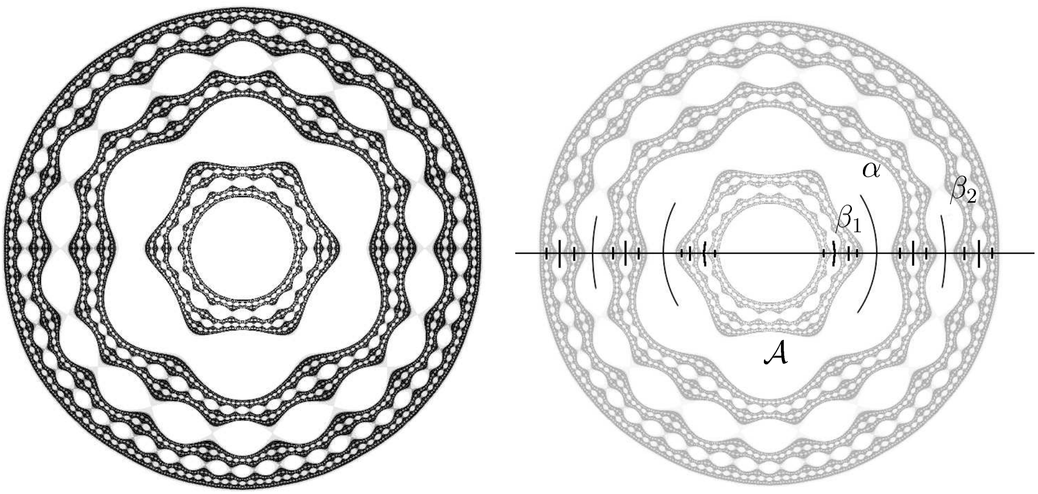

Figure 7: The Julia set for $F_{0.01}(z) = z^3 + 0.01/z^3$ (left) and the extended 0 ray (right).

this set is mapped two-to-one over itself. We then define the extended 1/2 ray to be the negative of the 0 ray. Then the full extended ray of angle 0 (or angle 1/2) is defined to be the union of the extended 0 and 1/2 rays. Note that this extended ray is now mapped two-to-one onto itself. The full 1/6 and 2/6 extended rays are symmetric copies of the extended 0 ray that pass through the other critical points and are each mapped two-to-one onto the full extended 0 ray. Then we may pull back these extended rays by appropriate inverses of F_λ to define the extended rays of angle θ where θ eventually lands on 0 or 1/2 under angle-tripling. Note that each of these extended rays passes through a Cantor set of points in the Julia set (i.e., a unique point on each circle in the Julia set), and each also has countably many attachments. See Figure 7.

All of the other extended rays for F_λ may then be defined as in the previous case using itineraries whose entries are $0, \ldots, 5$ and projected itineraries with entries defined mod 3. These rays are, as in the previous case, simple closed curves passing through 0 and ∞. For example, consider the extended 1/4 ray (with the 3/4 ray). We define this ray to be the set of all points that stay in either I_1 or I_4 for all iterates. One checks easily that the extended 1/4 (or 3/4) ray is just the imaginary axis together with the point at ∞. All of the rays that eventually map to the extended 1/4 ray will be simple closed curves without sets of attachments, as will any other extended ray that does not map to the 0 extended ray. One also checks immediately that each of these rays must pass through a pair of prepoles, so infinitely many of these extended rays cross each other as before.

4 A Parameter Drawn From a Sierpinski Hole

In this final section, we consider Sierpinski curve Julia sets drawn from the family

$$F_\lambda(z) = z^2 + \frac{\lambda}{z^2}.$$

For simplicity, we shall describe the structure of the extended rays for the single parameter value $\lambda = -1/16$. For this map there are 4 critical points located at $(-1)^{1/4}/2$ and two critical values located at $\pm i/2$. Then the critical values are both mapped to 0, so the critical orbits eventually escape and, by the Escape Trichotomy, $J(F_\lambda)$ is a Sierpinski curve. The critical circle is therefore mapped onto the portion of the imaginary axis between $\pm i/2$. The four prepoles are located on the real and imaginary axes at $\pm 1/2$ and $\pm i/2$ (which are also the critical values).

Consider the extension of the external 0 ray. The graph of F_λ shows that the real axis maps two-to-one over itself. See Figure 9. Thus, as before, the extended 0 ray is $\mathbb{R} \cup \{\infty\}$. Similarly, the extended 1/4 (or 3/4) ray is the imaginary axis. This is due to the fact that $F_{-1/16}(ix) = -F_{-1/16}(x)$. Since $F_{-1/16}(z)$ maps $\mathbb{R}$ two-to-one over itself, it follows that the imaginary axis is also mapped two-to-one over $\mathbb{R}$.

Next consider the extension of the 1/8 ray (and the 5/8 ray). Because this is a critical ray, its extension is more complicated (and different from the

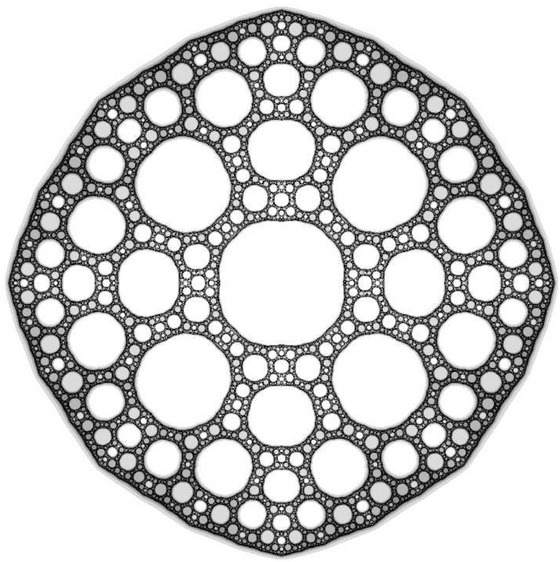

Figure 8: The Julia set for $F_{-1/16}(z) = z^2 - \frac{1}{16z^2}$. This is an example of a Sierpinski curve.

McMullen domain case). The external $1/8$ ray maps under angle doubling to the external $1/4$ ray. The entire $1/8$ ray (and also the $5/8$ ray) is a critical ray that extends from 0 to ∞ and so is mapped two-to-one over the portion of the imaginary axis extending from the critical value $i/2$ to ∞. Then the portion of the critical circle lying in the first quadrant is mapped onto the interval connecting 0 to $i/2$ on the imaginary axis. So we augment the $1/8$ ray to contain this quarter circle. We augment the $5/8$ ray in similar fashion. Then the full extended $1/8$ ray is the union of these two rays, i.e., the straight line containing the $1/8$ and $5/8$ straight rays together with the two quarter circles on the critical circle. Note that this extended ray does not map onto the entire extended $1/4$ ray. Since this extended ray contains two free critical points, it is only mapped onto the upper portion of the imaginary axis and ∞. In similar fashion we define the $3/8$ or $7/8$ extended ray. This ray is mapped onto the lower portion of the extended $1/4$ ray.

Now the first preimage of the extended $1/8$ ray is mapped two-to-one

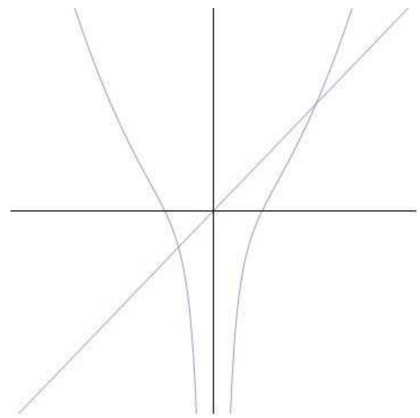

Figure 9: $F_{-1/16}(x) = x^2 - \frac{1}{16x^2}$.

onto the 1/8 ray, and so this ray will consist of a simple closed curve passing through 0 and ∞ as well as four attachments. Further preimages of this ray will have additional attachments, but, unlike the McMullen domain extended rays, there will only be finitely many such attachemnts in each case. And, as before, extended rays that are not preimages of the 1/4 ray are just simple closed curves through 0 and ∞. Note that all of these curves must again pass through a pair of prepoles on the critical circle as well as a Cantor set of points in the Julia set.

5 Conclusion

In this paper we have given three different examples of how external rays in the dynamical plane may be extended through a Cantor set of points in the Julia set as well as through countably many preimages of the basin at ∞. These extended rays partition the Julia set into Cantor set pieces that are mapped onto the image external ray via the shift map on two symbols. This gives a way to understand the complete dynamical behavior of these maps on the Julia set.

References

[1] Devaney, R. L. Structure of the McMullen Domain in the Parameter Space of Rational Maps. *Fundamenta Mathematicae* **185** (2005), 267-285.

[2] Devaney, R. L. The McMullen Domain: Satellite Mandelbrot Sets and Sierpinski Holes. *Conformal Geometry and Dynamics* **11** (2007), 164-190.

[3] Devaney, R. L. Baby Mandelbrot Sets Adorned with Halos in Families of Rational Maps. In *Complex Dynamics: Twenty-Five Years after the Appearance of the Mandelbrot Set.* American Math Society, Contemporary Math **396** (2006), 37-50.

[4] Devaney, R. L., Look, D. M., and Uminsky, D. The Escape Trichotomy for Singularly Perturbed Rational Maps. *Indiana University Mathematics Journal* **54** (2005), 1621-1634.

[5] Devaney, R. L. and Pilgrim, K. Dynamic Classification of Escape Time Sierpinski Curve Julia Sets. *Fundamenta Mathematicae* **202** (2009), 181-198.

[6] McMullen, C. The Classification of Conformal Dynamical Systems. *Current Developments in Mathematics.* International Press, Cambridge, MA, (1995) 323-360.

[7] Milnor, J. *Dynamics in One Complex Variable.* Third Edition. Annals of Mathematics Studies. Princeton University Press, (2006). 1999.

[8] Roesch, P. On Capture Zones for the Family $f_\lambda(z) = z^2 + \lambda/z^2$. In *Dynamics on the Riemann Sphere*. European Mathematical Society, (2006), 121-130.

[9] Whyburn, G. T. Topological Characterization of the Sierpinski Curve. *Fundamenta Mathematicae* **45** (1958), 320-324.

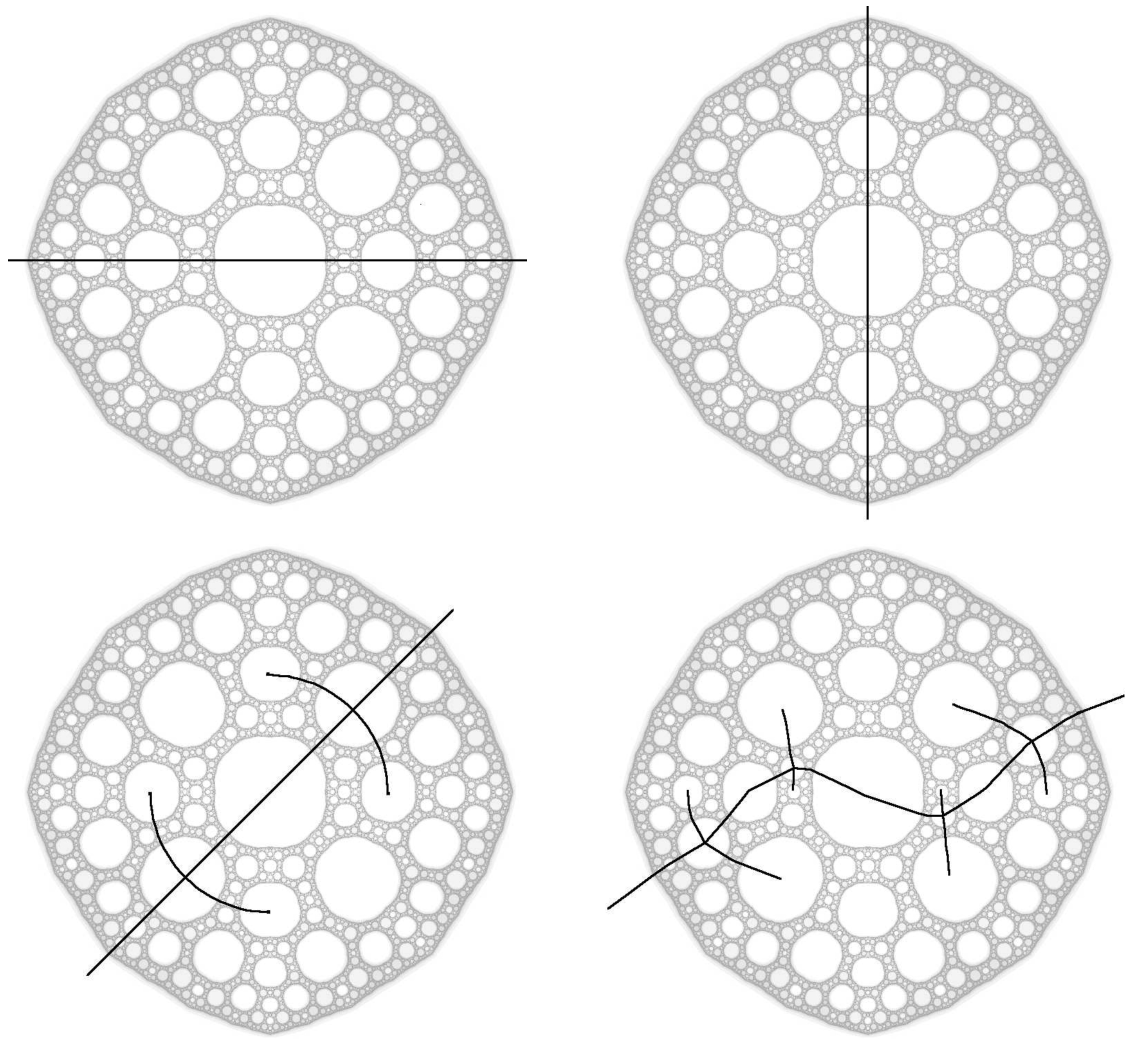

Figure 10: The 0 ray (top left), 1/4 ray (top right), 1/8 ray (bottom left), and 1/16 ray (bottom right).